Spin Seebeck power generators

Adam B. Cahaya, O. A. Tretiakov, and Gerrit E. W. Bauer

Citation: Appl. Phys. Lett. **104**, 042402 (2014);
View online: https://doi.org/10.1063/1.4863084
View Table of Contents: http://aip.scitation.org/toc/apl/104/4
Published by the American Institute of Physics

Spin Seebeck power generators

Adam B. Cahaya,[1] O. A. Tretiakov,[1] and Gerrit E. W. Bauer[2,3]
[1]*Institute for Materials Research, Tohoku University, Sendai 980-8577, Japan*
[2]*Institute for Materials Research and WPI-AIMR, Tohoku University, Sendai 980-8577, Japan*
[3]*Kavli Institute of NanoScience, TU Delft Lorentzweg 1, 2628 CJ Delft, The Netherlands*

(Received 24 November 2013; accepted 10 January 2014; published online 28 January 2014)

We derive expressions for the efficiency and figure of merit of two spin caloritronic devices based on the spin Seebeck effect (SSE), i.e., the generation of spin currents by a temperature gradient. The inverse spin Hall effect is conventionally used to detect the SSE and offers advantages for large area applications. We also propose a device that converts spin current into electric one by means of a spin-valve detector, which scales favorably to small sizes and approaches a figure of merit of 0.5 at room temperature. © *2014 AIP Publishing LLC*. [http://dx.doi.org/10.1063/1.4863084]

Thermoelectric phenomena[1] transform heat currents into electric power and vice versa. The Seebeck effect refers to the generation of an electromotive force (emf) by a temperature gradient,[2] while the production of a heat current by an applied charge current is called Peltier effect.[3] Thermoelectric power generators convert waste heat into electric energy with many potential applications.[4,5] The spin degree of freedom adds functionalities and may improve the efficiency of conventional thermoelectric devices.[6] The spin Seebeck effect (SSE) in the "longitudinal" configuration based on a ferromagnetic insulator[7] (FI) is especially promising. The SSE converts a temperature difference between the FI and a normal metal (N) contact into electric power[8,9] by pumping a spin current into the normal metal that, in turn, is converted into a transverse emf by the inverse spin Hall effect[10] (ISHE). The output power is proportional to the device area perpendicular to the temperature gradient. This scaling offers the opportunity to generate electricity by large-area coatings, using cheap materials.[11] Since here the paths of the charge and heat currents are perpendicular to each other, alternative strategies to enhance thermoelectric efficiency can be pursued.

In this Letter, we validate the efficiency of SSE based power generators. In addition to considering a device using the ISHE spin charge conversion, we propose harvesting electrical energy by a spin valve spin-filtering mechanism, employing metallic ferromagnets. The spin-valve based SSE power generator scales advantageously for the thermoelectric power generation in small structures, and multiple elements can be easily added for a higher output voltage, analogously to conventional thermopiles.

Thermoelectric generators produce electric power by the heat current that flows between hot and cold reservoirs at temperatures T_H and T_L, respectively. Its efficiency is a monotonic function of the dimensionless figure of merit ZT, where T is the average temperature $(T_H + T_L)/2$.[1] When $ZT \to \infty$, $\eta \to (T_H - T_L)/T_H = \eta_C$, where η_C is the maximum possible "Carnot" efficiency. Here, we derive $\eta(ZT)$ and ZT for the two types of generators driven by the SSE, taking into account the difference of the physical mechanism between the SSE and conventional thermoelectrics.[6]

In the spin Seebeck effect, the spin current flowing through the interface is caused by an imbalance of the spin pumping current due to magnetic thermal noise $\mathbf{J}_{sp}$, that is proportional to FI's magnon temperature T^m_{FI}, and a fluctuating spin current caused by thermal (Johnson-Nyquist) noise in the normal metal $\mathbf{J}_{fl}$ that is proportional to N's electron temperature.[12,13] Both currents on average are polarized parallel to the magnetization direction ($\hat{\mathbf{m}}$) and cancel each other at equilibrium. The net SSE spin current reads (indicating time average by $\langle \cdots \rangle$)[8]

$$J_S = \hat{\mathbf{m}} \cdot \langle \mathbf{J}_{sp} + \mathbf{J}_{fl} \rangle = L_S \left(T^m_{FI} - T^e_N \right), \tag{1}$$

where $L_S = \gamma \hbar G_r k_B / (2\pi e M_s V_c)$ is the interfacial response function, γ is the gyromagnetic ratio, G_r is the real part of spin mixing conductance, k_B is the Boltzmann constant, M_s is the saturation magnetization, e is the magnitude of electron's charge, and V_c is a magnetic coherence volume that depends on spin wave stiffness and weakly on temperature.[9] Adachi *et al.*[14] and Hoffman *et al.*[15] derived similar expressions by different methods. The magnitude of the real part of the mixing conductance G_r is well established for intermetallic interfaces[16] as well as interfaces with magnetic insulators.[17–19]

The interface temperature discontinuity depends sensitively on the device and material parameters.[20] In the limit of small interface heat resistance, the phonon temperature is continuous and governed by the coupled heat diffusion equation for the bilayer with many not very well-known parameters.[8,20,21] Here, we assume, for simplicity, a dominating thermal boundary resistance $R_K = 1/G_K$ (Kapitza resistance[22]), such that the magnon and phonon temperatures in the FI at the interface $(z = 0)$ are approximately the same,[20,23] $T^m_{FI}(z = 0^-) \approx T^p_{FI}(z = 0^-) = T_{FI}$, see Fig. 1. In this limit,

$$T_{FI} = T_N + R_K J_Q, \tag{2}$$

where T_N is the electron (and phonon) temperature of the normal metal at $z = 0^+$ and J_Q is the heat current through the interface. Since the spin contribution to the interface heat transport is comparably small, the Kapitza resistance R_K is dominated by phonon transport.[8,20]

The heat flow through the system is partly converted into a spin current at the interface that subsequently has to be transformed into electric energy. The coupling between heat and spin over the FI|N interface can be written in the form of a linear response matrix relation to the driving forces, viz.,

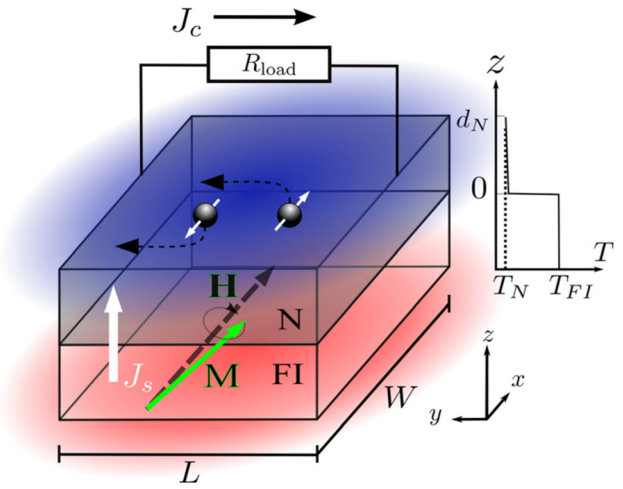

FIG. 1. A schematic view of the spin Seebeck power generator based on the ISHE. A bilayer of ferromagnetic insulator and normal metal with a low interface heat conductance pumps a spin current J_s into N. Then J_s is converted into a transverse charge current J_c by means of the ISHE.

the spin accumulation μ_s in the normal metal and temperature difference $\Delta T = T_N - T_{FI}$, leading to the spin J_s and averaged heat $J_Q = \left(J_Q^{\rm IN} + J_Q^{\rm OUT}\right)/2$ current responses

$$\begin{pmatrix} J_s \\ J_Q \end{pmatrix} = G_S \begin{pmatrix} 1 & S_S \\ \Pi_S & G_K/G_S + S_S\Pi_S \end{pmatrix} \begin{pmatrix} -\mu_s/2e \\ -\Delta T \end{pmatrix}. \quad (3)$$

Here, G_S is the interface spin injection conductance,[24,25] that generates backflow of the spin Seebeck spin current, $S_S = \left(\mu_s/(2e\Delta T)\right)_{J_s=0} = L_S/G_S$ is the spin Seebeck coefficient, and $G_K = -\left(J_Q/\Delta T\right)_{J_s=0}$ is the Kapitza conductance (inverse of the Kapitza resistance $G_K = 1/R_K$). The spin current is positive when $\Delta T < 0$ and $\mu_s < 0$, so $G_S, S_S > 0$. The spin Peltier coefficient $\Pi_S = S_S T$ due to Onsager reciprocity, where $T = (T_N + T_{FI})/2$.

We first consider the efficiency of a SSE generator with spin-charge conversion by the ISHE when connected to an external load resistance $R_{\rm load}$ that utilizes the electric energy. The basic setup is shown in Fig. 1. Equation (3) defines the spin and heat currents through the FI|N interface. The transverse electric current density $\mathbf{j}_c$ generated by the ISHE inside N at distance z from interface is

$$\mathbf{j}_c(z) = \theta_{\rm SH} j_s(z) \hat{\mathbf{z}} \times \hat{\mathbf{m}}, \quad (4)$$

where $j_s(z)\hat{\mathbf{z}}$ is the spin-current density direction vector (in units of A/m^2), $\hat{\mathbf{m}}$ is its polarization, and $\theta_{\rm SH}$ is the spin Hall angle. For $\hat{\mathbf{m}} = \hat{\mathbf{x}}$, the charge current and emf are $\mathbf{j}_c = j_c\hat{\mathbf{y}}$ and $\nabla\mu = e\mathbf{E} = \hat{\mathbf{y}}\partial_y\mu_c$. In the presence of spin flips, a spin accumulation profile $\nabla\mu_s = \hat{\mathbf{z}}\partial_z\mu_s$ builds up at the interface. It obeys the spin-diffusion equation $\partial_z^2\mu_s = \mu_s/\lambda^2$, where λ is the spin-flip diffusion length in N. The charge and spin current densities in N therefore read

$$\begin{pmatrix} j_c \\ j_s \end{pmatrix} = -\sigma_N \begin{pmatrix} 1 & \theta_{\rm SH} \\ -\theta_{\rm SH} & 1 \end{pmatrix} \begin{pmatrix} \partial_y\mu_c/e \\ \partial_z\mu_s/(2e) \end{pmatrix}. \quad (5)$$

Spin current conservation at the boundaries $z = 0, d_N$ gives $j_s(z=0) = J_s/(WL)$ from Eq. (3) and $j_s(d_N) = 0$, where L is the length of N in the direction of the ISHE current, and W is the width of the FI|N bilayer (see Fig. 1). The solution of the spin-diffusion equation

$$\frac{\mu_s}{2e} = \frac{\theta_{\rm SH} V \frac{\lambda}{L}\left(G_S \sinh\frac{z}{\lambda} + G_N \cosh\frac{z}{\lambda}\right)}{G_S \cosh\frac{d_N}{\lambda} + G_N \sinh\frac{d_N}{\lambda}} - \frac{\left(\theta_{\rm SH} G_N V \frac{\lambda}{L} + G_S S_S \Delta T\right)\cosh\frac{d_N - z}{\lambda}}{G_S \cosh\frac{d_N}{\lambda} + G_N \sinh\frac{d_N}{\lambda}} \quad (6)$$

depends on the spin conductance $G_N = \sigma_N WL/\lambda$ and the induced transverse voltage $V = -L\partial_y\mu_c/e$. The integrated transverse charge current J_c in N then reads

$$J_c = -\frac{G_N\lambda}{L}\left[\frac{\theta_{\rm ISHE} G_S S_S \Delta T \tanh\frac{d_N}{2\lambda}}{G_S \coth\frac{d_N}{\lambda} + G_N} + \frac{d_N V}{L} + \frac{\theta_{\rm ISHE}^2 \lambda V}{L}\frac{G_S + 2G_N \tanh\frac{d_N}{2\lambda}}{G_S \coth\frac{d_N}{\lambda} + G_N}\right]. \quad (7)$$

The SSE generator is a battery with internal resistance $R_{\rm ISHE}^{\rm SSE} \propto L/W$ and a maximum output voltage $V_{\rm ISHE}^{\rm SSE}$,[26] see Fig. 2, that is

$$J_c = \frac{V_{\rm ISHE}^{\rm SSE} - V}{R_{\rm ISHE}^{\rm SSE}}, \quad (8)$$

$$V_{\rm ISHE}^{\rm SSE} = -R_{\rm ISHE}^{\rm SSE}\frac{\theta_{\rm SH}\sigma_N W G_S S_S \Delta T \tanh\frac{d_N}{2\lambda}}{G_S \coth\frac{d_N}{\lambda} + G_N} \propto L, \quad (9)$$

$$\frac{1}{R_{\rm ISHE}^{\rm SSE}} = \frac{\sigma_N W\lambda}{L}\left(\frac{d_N}{\lambda} + \theta_{\rm SH}^2 \frac{G_S + 2G_N \tanh\frac{d_N}{2\lambda}}{G_S \coth\frac{d_N}{\lambda} + G_N}\right). \quad (10)$$

The voltage drop over the load resistance $R_{\rm load}$ is

$$V = \frac{R_{\rm load}}{R_{\rm load} + R_{\rm ISHE}^{\rm SSE}} V_{\rm ISHE}^{\rm SSE} \propto L. \quad (11)$$

The thermally generated electric power $\mathcal{W} = J_Q^{\rm IN} - J_Q^{\rm OUT}$ dissipated in the load resistance

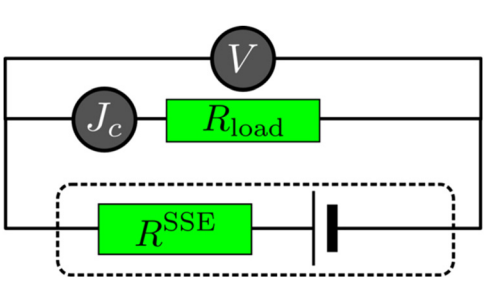

FIG. 2. An effective circuit for the spin Seebeck power generators with internal resistance $R^{\rm SSE}$. Current J_c and voltage V on external load with $R_{\rm load}$ are measured by ideal volt and ampere meters.

$$\mathcal{W} = \frac{V^2}{R_{\rm load}} = R_{\rm load}\left(\frac{V_{\rm ISHE}^{\rm SSE}}{R_{\rm load}+R_{\rm ISHE}^{\rm SSE}}\right)^2 \tag{12}$$

scales with the device area WL. The maximum output voltage $V_{\rm ISHE}^{\rm SSE}$ when $R_{\rm load}\to\infty$ is proportional to the sample length L. $V_{\rm ISHE}^{\rm SSE}\sim 1/d_N$ for large d_N, since the emf is short-circuited by the non-active conducting region. When $d_N \ll \lambda$, the voltage output vanishes with the gradient of the spin accumulation.

The efficiency $\eta^{\rm SSE} = \mathcal{W}/|J_Q|$ can be expressed in a form similar to conventional thermoelectrics[1]

$$\eta^{\rm SSE} = \frac{|\Delta T|}{T_H}\frac{\sqrt{1+(ZT)^{\rm SSE}}-1}{\sqrt{1+(ZT)^{\rm SSE}}+1-|\Delta T|/T_H} \tag{13}$$

in terms of figure of merit $(ZT)^{\rm SSE}$ that can be obtained by maximizing $\eta^{\rm SSE}$ with respect to $R_{\rm load}$, i.e., by impedance matching, leading to

$$(ZT)_{\rm ISHE}^{\rm SSE} = \frac{4\theta_{\rm SH}^2 e^{-d_N^{\rm opt}/\lambda} G_N S_S^2 T/G_K}{\left(1+\frac{G_N}{G_S}\right)\left(1+\frac{G_N}{G_S}+\frac{G_N S_S^2 T}{G_K}\right)}. \tag{14}$$

Here, the thickness $d_N^{\rm opt}$ for the optimal spin-charge conversion is given by the (positive) solution of the equation

$$\frac{d_N^{\rm opt}}{\lambda}+\theta_{\rm SH}^2 = \frac{1}{2}\sinh\frac{d_N^{\rm opt}}{\lambda}. \tag{15}$$

We can now estimate the figure of merit for the yttrium iron garnet (YIG)|Pt system $(ZT)_{\rm ISHE}^{\rm SSE}$. The spin Seebeck coefficient has the universal value $S_S \approx k_B/(1.3\times e) \approx 65\,\mu{\rm VK}^{-1}$.[25] With[19] $G_r/A = (e^2/h)10^{19}\,{\rm m}^{-2} = 4\times10^{14}\Omega^{-1}{\rm m}^{-2}$, we find (here and in the following at room temperature) $L_S/A \sim 4\times10^9\ {\rm AK}^{-1}{\rm m}^{-2}$. The spin conductance $G_S = L_S/S_S$ governs the spin current injected back into FI by the spin accumulation and is estimated for the YIG|Pt interface to be $G_S/A \sim 6\times10^{13}\,\Omega^{-1}{\rm m}^{-2}$, i.e., much smaller than the spin conductance of Pt: $G_N/A = 10^{15}\,\Omega^{-1}\,{\rm m}^{-2}$ for[19] $\lambda = 1.5\,{\rm nm}$ and $\rho_{Pt} = 500\,{\rm n\Omega m}$. Limit $G_S/G_N\to 0$ leads to the simplification

$$(ZT)_{\rm ISHE}^{\rm SSE} \to 4\theta_{\rm SH}^2 e^{-d_N^{\rm opt}/\lambda}\frac{L_S^2 T}{G_N}\frac{1}{G_K+G_S S_S^2 T}. \tag{16}$$

It shows that $(ZT)_{\rm ISHE}^{\rm SSE}$ is invariant with respect to the sample area. We can estimate its value using[19] $\lambda = 1.5\,{\rm nm}$ and $\theta_{\rm SH} = 0.1$, as well as the phonon contribution to the Kapitza conductance[20] $G_K^{\rm (ph)}/A = 1.6\times10^8\,{\rm Wm}^{-2}\,{\rm K}^{-1}$, which corresponds to about 40 nm of bulk YIG and is larger than the spin contribution[20] $G_K^{\rm (m)}/A \sim 0.5\times10^8\,{\rm Wm}^{-2}{\rm K}^{-1}$. This leads to $L_S^2T/(G_NG_K)\sim 0.025$ and $(ZT)_{\rm ISHE}^{\rm SSE}\sim 10^{-4}$ for the optimum width of $d_N^{\rm opt} = 2.16\,\lambda$.

We now turn to the alternative SSE power generator in which the thermal spin-motive force generates an electromotive force by means of ferromagnetic metal (FM) contacts, viz., by the spin valve effect. The N layer is now a metal with a long spin-flip diffusion length such as Cu. As shown in Fig. 3, the spin current in this case is injected into

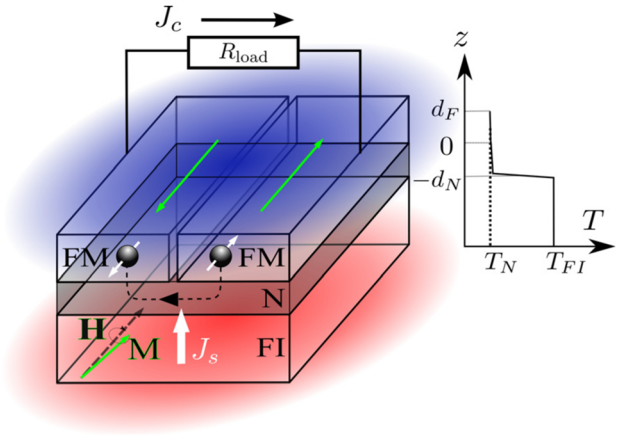

FIG. 3. A schematic view of the spin-valve based spin Seebeck power generator. Two antiparallel FM layers are added to the FI|N bilayer device in Fig. 1. The spin accumulation in N drives a charge current through the metallic spin valve, thereby generating a voltage over the load resistance.

the N layer of a lateral metallic spin valve with ferromagnetic contacts in an antiparallel configuration collinear to the magnetization of the magnetic insulator. The spin accumulation injected thermally into the N spacer therefore generates a voltage difference between the contacts. The FM|N contact areas are A and that of the FI|N contact is approximately $2A$.

We assume that the spin-flip diffusion length is larger than the sample dimensions such that the spin accumulation is constant in N. The charge-spin linear response relations at the interface of the N|FM interface with conductance G_I (including the magnetically active thickness of the bulk ferromagnet) can be written as

$$\begin{pmatrix} j_c^{(m)} \\ j_s^{(m)} \end{pmatrix} = \frac{G_I}{eA}\begin{pmatrix} 1 & mP \\ mP & 1 \end{pmatrix}\begin{pmatrix} \mu^{(m)}(0)-\mu^N \\ \left(\mu_s^{(m)}(0)-\mu_s^N\right)/2 \end{pmatrix}, \tag{17}$$

where $P \equiv (G_I^\uparrow - G_I^\downarrow)/(G_I^\uparrow + G_I^\downarrow)$ is the spin polarization of the N|FM contact, μ^N and μ_s^N are the electrochemical potential and spin accumulation in N, $\mu^{(m)}$ and $\mu_s^{(m)}$ are the electrochemical potential and spin accumulation in FM, and the superscript $m = \pm$ corresponds to a contact with magnetization parallel (+) or antiparallel (−) to that of the FI.

Assuming zero spin accumulation on the other side of the FM contact and conservation of spin current in N, $J_s^N = J_s^0 + \sum_\pm J_s^\pm(0) = 0$

$$\frac{\mu_s^N}{2e} = \frac{-G_S S_S \Delta T - P G_I V}{G_S + 2G_I}, \tag{18}$$

$$J_c = \frac{P S_S \Delta T/G_I}{1+2G_I/G_S} - \frac{G_I V}{2}\frac{1+2(1-P^2)G_I/G_S}{1+2G_I/G_S}, \tag{19}$$

where the induced voltage $V = (\mu^- - \mu^+)/e$. The effective electric circuit for the spin-valve based generator is again given by Fig. 2 with internal resistance $R_{\rm SV}^{\rm SSE}$ and maximum voltage $V_{\rm SV}^{\rm SSE}$

$$V_{\rm SV}^{\rm SSE} = \frac{2PS_S\Delta T}{1+2(1-P^2)G_I/G_S}, \tag{20}$$

$$R_{\mathrm{SV}}^{\mathrm{SSE}} = \frac{2}{G_I}\frac{1+2G_I/G_S}{1+2(1-P^2)G_I/G_S}. \tag{21}$$

The optimal figure of merit $(ZT)_{\mathrm{SV}}^{\mathrm{SSE}}$ is obtained again by maximizing the efficiency η^{SSE} with respect to R_{load}

$$(ZT)_{\mathrm{SV}}^{\mathrm{SSE}} = \frac{2P^2 G_I S_S^2 T/G_K}{\left(1+\frac{2G_I}{G_S}\right)\left[1+2(1-P^2)\left(\frac{G_I}{G_S}+\frac{G_I S_S^2 T}{G_K}\right)\right]}. \tag{22}$$

For an intermetallic interface, $G_S \ll G_I$[27] and

$$\lim_{G_S\to 0}(ZT)_{\mathrm{SV}}^{\mathrm{SSE}} = \frac{P^2}{1-P^2}\frac{G_S}{2G_I}\frac{G_S S_S^2 T}{G_K}. \tag{23}$$

In the limit of a half-metal, this expression appears to diverge, but when we first take $P \to 1$ and then $G_S/G_I \to 0$

$$\lim_{G_S/G_I\to 0}\lim_{P\to 1}(ZT)_{\mathrm{SV}}^{\mathrm{SSE}} = \frac{G_S S_S^2 T}{G_K} \sim 0.5, \tag{24}$$

the result looks similar to the figure of merit for conventional thermoelectrics. The numerical estimate is obtained for[20] $G_K/A \sim 1.6\times 10^8\,\mathrm{m^{-2}K^{-1}}$ and[19] $G_r/A \sim 4\times 10^{14}\,\Omega^{-1}\mathrm{m}^{-2}$.

To summarize, we consider two schemes of thermoelectric power generators based on the spin Seebeck effect. We estimate their figures of merit $(ZT)^{\mathrm{SSE}}$ under the assumption that the total heat conductance is limited by the FI|N interface. This assumption importantly simplifies the model, but since the Kapitza interface conductance has not yet been measured for YIG|metal interfaces, also introduces uncertainties. The output voltage of the SSE-ISHE device is proportional to sample length L perpendicular to the FI's magnetization and temperature gradient (Fig. 1), while the power scales with the area. Therefore, this scheme has an advantage for large area devices, but $(ZT)_{\mathrm{ISHE}}^{\mathrm{SSE}}$ is small since it is limited by $\theta_{\mathrm{SH}}^2 \exp(-d_N/\lambda)$. A spin valve can convert spin into charge current as well, offering the possibility to enhance ZT considerably. The scale independence of the output voltage in spin-valve SSE devices can be useful for micro- and nanoscale applications, since the output voltage does not decrease when down-scaling the device. Experiments demonstrating the SSE by a spin valve are highly desirable since they would shed light on the role of interface proximity or spin-orbit interaction effects that might exist for YIG|Pt but not for YIG|Cu.[28] The present modelling is also applicable for other devices, such as spin Seebeck-assisted magnetic random access memories.[29]

We thank E. Saitoh, K. Uchida, J. Flipse, and J. Xiao for insightful discussions. A.B.C. was supported by a Japanese Ministry of Education Culture, Sports, Science and Technology (MEXT) Scholarship Grant. We acknowledge support by the Grants-in-Aid for Scientific Research (Nos. 25800184, 25220910, and 25247056), the DFG via SPP 1538 "Spin Caloric Transport", the EU RTN Spinicur and DAAD SpinNet.

[1]M. Sakata, *Thermoelectric Energy Conversion: Theory and Applications* (Shokabo, Tokyo, 2005).
[2]T. J. Seebeck, Abh. Dtsch. Akad. Wiss. Berlin **265**, 1822 (1823).
[3]J. C. Peltier, Ann. Chim. **56**, 371 (1834).
[4]C. B. Vining, Nature Mater. **8**, 83 (2009).
[5]J. P. Heremans, M. S. Dresselhaus, L. E. Bell, and D. T. Morelli, Nat. Nanotechnol. **8**, 471 (2013).
[6]G. E. W. Bauer, E. Saitoh, and B. J. van Wees, Nature Mater. **11**, 391 (2012).
[7]K. Uchida, J. Xiao, H. Adachi, J. Ohe, S. Takahashi, J. Ieda, T. Ota, Y. Kajiwara, H. Umezawa, H. Kawai, G. E. W. Bauer, S. Maekawa, and E. Saitoh, Nature Mater. **9**, 894 (2010).
[8]J. Xiao, G. E. W. Bauer, K. Uchida, E. Saitoh, and S. Maekawa, Phys. Rev. B **81**, 214418 (2010).
[9]J. Xiao, G. E. W. Bauer, K. Uchida, E. Saitoh, and S. Maekawa, Phys. Rev. B **82**, 099904(E) (2010).
[10]For a review, see A. Hoffmann, IEEE Trans. Magn. **49**, 5172 (2013).
[11]A. Kirihara, K. Uchida, Y. Kajiwara, M. Ishida, Y. Nakamura, T. Manako, E. Saitoh, and S. Yorozu, Nature Mater. **11**, 686 (2012).
[12]J. Foros, A. Brataas, Y. Tserkovnyak, and G. E. W. Bauer, Phys. Rev. Lett. **95**, 016601 (2005).
[13]J. Xiao, G. E. W. Bauer, S. Maekawa, and A. Brataas, Phys. Rev. B **79**, 174415 (2009).
[14]H. Adachi, J. Ohe, S. Takahashi, and S. Maekawa, Phys. Rev. B **83**, 094410 (2011).
[15]S. Hoffman, K. Sato, and Y. Tserkovnyak, Phys. Rev. B **88**, 064408 (2013).
[16]A. Brataas, G. E. W. Bauer, and P. J. Kelly, Phys. Rep. **427**, 157 (2006).
[17]X. Jia, K. Liu, K. Xia, and G. E. W. Bauer, Europhys. Lett. **96**, 17005 (2011).
[18]C. Burrowes, B. Heinrich, B. Kardasz, E. A. Montoya, E. Girt, Y. Sun, Y.-Y. Song, and M. Wu, Appl. Phys. Lett. **100**, 092403 (2012).
[19]M. Weiler, M. Althammer, M. Schreier, J. Lotze, M. Pernpeintner, S. Meyer, H. Huebl, R. Gross, A. Kamra, J. Xiao, Y. Chen, H. Jiao, G. E. W. Bauer, and S. T. B. Goennenwein, Phys. Rev. Lett. **111**, 176601 (2013).
[20]M. Schreier, A. Kamra, M. Weiler, J. Xiao, G. E. W. Bauer, R. Gross, and S. T. B. Goennenwein, Phys. Rev. B **88**, 094410 (2013).
[21]D. J. Sanders and D. Walton, Phys. Rev. B **15**, 1489 (1977).
[22]G. L. Pollack, Rev. Mod. Phys. **41**, 48 (1969).
[23]M. Agrawal, V. I. Vasyuchka, A. A. Serga, A. D. Karenowska, G. A. Melkov, and B. Hillebrands, Phys. Rev. Lett. **111**, 107204 (2013).
[24]S. A. Bender, R. A. Duine, and Y. Tserkovnyak, Phys. Rev. Lett. **108**, 246601 (2012).
[25]H. Jiao, J. Xiao, and G. E. W. Bauer (unpublished).
[26]A. B. Cahaya, O. A. Tretiakov, and G. E. W. Bauer (unpublished).
[27]J. Hamrle, T. Kimura, Y. Otani, K. Tsukagoshi, and Y. Aoyagi, Phys. Rev. B **71**, 094402 (2005).
[28]S. Y. Huang, X. Fan, D. Qu, Y. P. Chen, W. G. Wang, J. Wu, T. Y. Chen, J. Q. Xiao, and C. L. Chien, Phys. Rev. Lett. **109**, 107204 (2012).
[29]N. N. Mojumder, D. W. Abraham, K. Roy, and D. C. Worledge, IEEE Trans. Magn. **48**, 2016 (2012).